Conversion of Light to Electricity by Photoinduced Reversible pH Changes and Biomimetic Nanofluidic Channels

*Liping Wen, Ye Tian, Yongli Guo, Jie Ma, Weida Liu, and Lei Jiang**

Inspired by living systems that have the inherent skill to convert solar energy into bioelectric signals with their light-driven cross-membrane proton pump, a photoelectric conversion system that can work in alkaline conditions based on photoinduced reversible pH changes by malachite green carbinol base and a smart gating hydroxide ion-driven nanofluidic channel is demonstrated. In this system, solar energy can be considered as the only source of cross-membrane proton motive force that induces diffusion potential and photocurrent flowing through the external circuit. The conversion performances are 0.00825% and 36%, which are calculated from the photoelectric conversion and Gibbs free energy diffusion, respectively. The results suggest that electric power generation and performance could be further optimized by selecting appropriate photosensitized molecules and enhancing the surface-charge density as well as adopting the appropriate channel size. This facile, cost-efficient, and environmentally friendly photoelectric conversion system has potential applications for future energy demands such as production of power for in vivo medical devices.

1. Introduction

Ions that flow through a channel and induce a power generation have widely been found in life.[1] When such a system is stimulated, electrical energy can be harvested from ambient environment.[2] However, these channels in living systems can only work in the environment of lipid membranes, which makes their applications out of living systems difficult. Recent advances in fabrication and application of artificial nanochannels have aroused great interest because of their similar functions to biological nanochannels but would be stable in a variety of conditions, such as temperature, pH, mechanical stress, etc.[3] This advantage brings them potential applications in sensing,[4] filtrating,[5] and energy conversion.[2,6]

In a synthetic nanochannel system, counter ions are transported in a confined region with an electrical double layer under certain driving forces, such as concentration and pressure gradients, generating diffusion potential and streaming current. For example, Dekker reported electrokinetic energy conversion system using a synthetic nanochannel.[2d,6b–d] He estimated that the developed electrokinetic energy conversion device could reach a maximum efficiency of 12% if simple monovalent ions were used in aqueous solution. Wang and his coworkers investigated the efficiency of power generation with a single conical track-etched nanopore.[7] They found the performance of power generation was greatly correlated with the type and the concentration of electrolyte inside the nanopore. In 2010, we developed a fully abiotic single-pore nanofluidic energy-harvesting system[2c] whose power density could be enhanced by one to three orders over previous ion-exchange membranes. Most recently, Gillespie reported that the layering of large ions at the wall/liquid interface of nanofluidic channels could be used to achieve high efficiency (possibly >50%) in the conversion of hydrostatic energy into electrical power.[2e] It is obvious from the preceding example that most of reported energy conversion systems based on nanofluidic channels are dependent on external power supply. Solar energy as a clean and sustainable resource would act perfectly as such an external power supply. As a result, nanochannel-based energy conversion systems using solar energy have recently aroused intense research interests.

As an example of solar energy conversion in living system, retina only needs one cyclic process which is different from the photosynthesis in green plants.[8] Sunlight can be absorbed and converted to electronic excitation signal with the help of their light-driven proton pump without complication of the two photosystems and water oxidation. Inspired by the retina, scientists tried to use this biological light driven proton pump molecule to construct photoelectric conversion systems by dissolving it in solutions[9] or depositing it on electrodes,[10] from which they could produce a transient signal that behaved similarly to normal photoreceptors. Considering the weak power generation

Dr. L. Wen, Dr. Y. Tian, Dr. J. Ma, W. Liu, Prof. L. Jiang
Beijing National Laboratory for Molecular Sciences (BNLMS)
Key Laboratory of Organic Solids
Institute of Chemistry
Chinese Academy of Sciences
Beijing 100190, P. R. China
E-mail: jianglei@iccas.ac.cn

Y. Guo, Prof. L. Jiang
Key Laboratory of Bio-Inspired Smart Interfacial Science and Technology of Ministry of Education
School of Chemistry and Environment
Beihang University
Beijing 100191, P. R. China

DOI:10. 1002/adfm.201203259

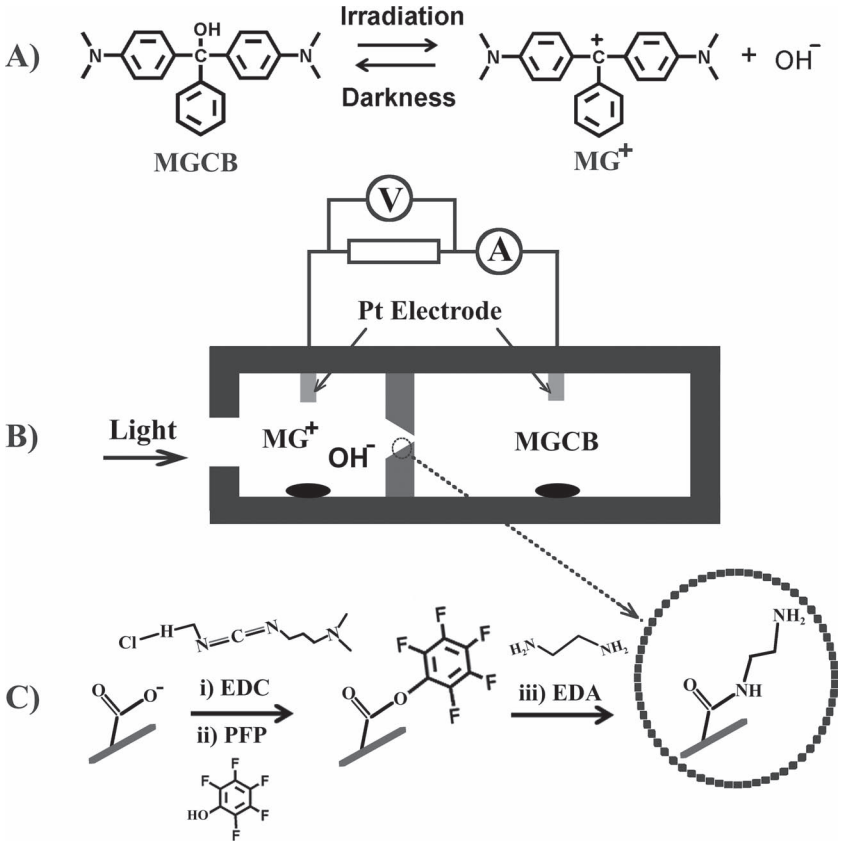

Scheme 1. Schematic sketch of the photoelectric conversion system. A) Light-dependent MGCB equilibrium taking place in a photoeclectrochemical cell. B) The experimental setup that could be irradiated from one side of the cell. C) The chemical modification strategy for converting the carboxyl groups into amino terminated groups.

and poor stability of biomolecules, issues of interfacing the photoelectric conversion systems with biological light-driven proton pump led to the development of novel photoelectric conversion systems with biomimetic analogues. For example, inspired by the photoelectric conversion of retina, we previously reported a novel photoelectric conversion system with a smart gating proton-driven nanochannel and photoinduced proton pump, 8-hydroxypyrene-1,3,6-trisulfonate (HPTS)[2b] that could realize the function of protons release and uptake under the condition of irradiation and darkness. Under irradiation, the generated protons would transport across the smart gating nanochannels membrane and resulted in charge imbalance on both sides of membrane which contributed to the diffusion potential and photocurrent generation. However, such a system can only work in the acidic environment, which greatly reduces it application in alkaline or full pH 1 to 14 conditions. In order to apply such a photoelectric conversion system in alkaline condition, Here, we further develop the concept of bio-inspired photoelectric conversion system by using a photo-induced reversible pH changes molecule, malachite green carbinol base (MGCB)[11] and biomimetic smart gating hydroxide ion-driven nanofluidic channels. Compared to the system with HPTS, this photoelectric conversion system has the advantages that it can be worked in alkaline condition with the rapidly dissociation proceeds in high quantum yield[12] and high photoelectric conversion efficiency.

2. Results and Discussion

The photoelectric conversion system, which is illustrated in **Scheme 1**, is composed of three main components: 1) a photoelectrochemical cell (PEC) that can be irradiated from one side with platinum electrodes whose structure was similar to the PEC made by Kamo (Scheme 1A);[9] 2) a functionalized nanochannel membrane that was prepared by modifying amino ($-NH_2$) terminated groups (ethylenediamine) onto the inner surface of an ion track-etched conical nanochannel (see Experimental Section and Supporting Information Figure S1); and 3) a light-induced hydroxide ion emitter, molecular malachite green carbinol base (MGCB).[11] The pH of the testing solution was about 6.9–8.5, causing the surface of the amino ($-NH_2$) terminated group-functionalized conical nanochannel to be positively charged.[13] The charged nanochannel exhibited ionic current rectification behavior, because the asymmetry property preferentially transported anions from the small opening (tip) towards the large opening (base) side of the channel even when the electrolyte was the same for the two sides (see Supporting Information Figure S2).[14] The original diameter at the base side of the naked conical nanochannel was about 500 nm (measured by scanning electron microscopy), and the diameter at the tip side was calculated to be ≈10 nm by an electrochemical measurement. When the MGCB molecules were irradiated by UV light, they would release OH^- and malachite green cations (MG^+), as well as showing an obvious color change, leading to an increase of the pH value (pH = 8.5). Then the generated OH^- would transport across the membranes under the force of concentration gradients from the irradiation side of the cell to the darkness side, and resulted in charge imbalance on both sides of membrane which contributed to the diffusion potential (E_{dif}). If the two platinum electrodes were connected with metal wires, electrons (I_p) that generated by redox reactions on platinum electrodes would flow from external circuit whose mechanism was similar to the photoelectric conversion systems with HPTS[2b] and bacteriorhodopsin.[10b,10d,15] The used instruments and the measurement techniques are the same with our previous work.[2b] Once the light cut off, the MG^+ will recombine with the OH^- ions and recover to the original MGCB molecules (Scheme 1A). The multicycle of pH changes of MGCB was shown in the Supporting Information (Figure S3).

The typical response properties of the photoelectric conversion measured under irradiation and in darkness were shown in **Figure 1**. We found that the E_{dif} and the I_p tended to be constant when the system was in darkness. Under irradiation, the photochemical reactions occurred immediately, which resulted in an E_{dif} and an output I_p. The maximum values can be obtained within 5 min. The values are 56.8 mV and 1.55 μA/cm^2,

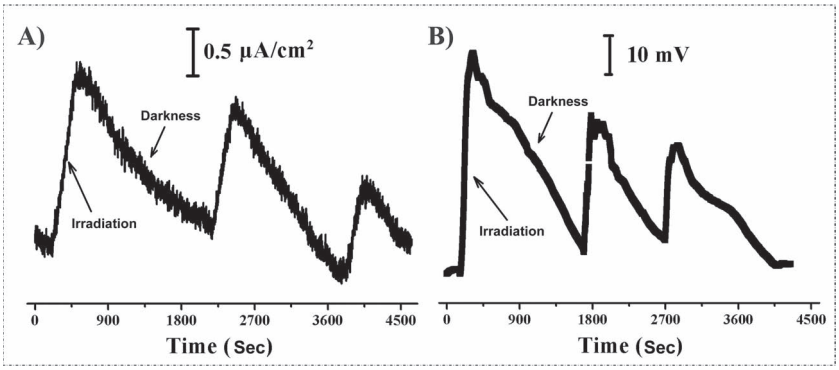

Figure 1. Photoresponse of the faradaic photocurrent and membrane potential to alternating UV irradiation and darkness. An amino-terminator-functionalized nanochannel membrane was used in this photoelectric conversion system. The electrolyte was 0.24 mM MGCB solution (T = 25 °C, I_s = 375 mW/cm^2). Sample: base ≈ 500 nm, tip ≈ 10 nm, before chemical modification.

respectively (absolute values). When the light was removed, both E_{dif} and I_p decreased rapidly but they could not recover to the original state. If the MGCB molecule was irradiated again, less hydroxide ion was induced in the solution, the second peak would arise but they were weaker than the peak in the first cycle. Further research is ongoing to achieve continuous power supply.

Different from the energy conversion system with HPTS and bacteriorhodopsin, MGCB can release and uptake hydroxide ions with the help of a surfactant, cetyltrimethylammonium bromide (CTAB) which can make MGCB dissolve easily into the water. Moreover, the original pH in the MGCB solutions can also influence the pH changes and the output power generation. The influence of the CTAB concentration and the original pH in MGCB solution were studied and the results were given in **Table 1**, **2**. As shown in Table 1, both the photocurrent and the membrane potential are influenced by the concentration of CTAB, because the changes of pH and solution resistance are decided partly by the amounts of CTAB in MGCB solutions. When the CTAB concentration is low, such as 35 mM, few of MGCB can be dissolved into solution and the photoinduced pH changes cannot be obtained in a wide range, resulting in very weak photocurrent and membrane potential. On the contrary, too much amounts of CTAB in the MGCB solutions cannot produce very high power generation, the reason is that the interaction between the cations and anions generated by CTAB and MGCB will impede ion diffusion along with concentration gradients.[16] In our experiment, with a CTAB concentration of 50 mM, we obtained large photocurrent and membrane potentials; the values were around 1.54 μA/cm^2 and 56.84 mV, respectively. The photocurrent and membrane potential changes induced by the first irradiation are summarized in Table 2, showing photo-induced current and potential changes under different pH conditions. We found the values of photocurrent and membrane potential measured at neutral pH condition was obviously higher than the values measured at the conditions of acidic and alkaline environments. This may be ascribed to the high pH that can accelerate the reverse reaction, as shown in Scheme 1A, while the protons at low pH conditions can neutralize the generated hydroxide ions and form proton gradients, which cannot transport the amino terminated nanochannel easily.

Table 1. Influence of the concentration of CTAB on power generation.

CTAB [mM]	35.0	50.0	100.0
I (μA/cm^2)	0.269691	1.53656	0.600605
V(mV)	27.3393	56.84036	33.8370

Table 2. Influence of the pH of original MGCB solution on power generation.

pH	4.0	7.0	12.0
I(μA/cm^2)	0.107442	1.53656	0.36253
V(mV)	19.9509	56.84036	17.0152

The time-course changes of membrane potentials were shown in **Figure 2**, which varied with UV irradiation at different concentration of MGCB solutions with a fixed incident light intensity and environment temperature. We found that the E_{dif} tended to be a constant when the system was in dark environment. Under UV irradiation, MGCB molecules released hydroxide ions which transport across the nanochannel under the hydroxide ion gradient. Then the E_{dif} shifted in the negative direction (positive terminal of ammeters all connected to the platinum electrode that input the dark side of PEC) and gradually reached the maximum value. Furthermore, the diffusion rate decreased with the increasing concentration of MGCB molecules, and the maximum E_{dif} did not reach at the most concentrated MGCB solution either, which should be ascribed to the interaction of ions in the process of hydroxide diffusion.

To better understand the dependence of E_{dif} and I_p on MGCB molecule, different concentrations of MGCB solutions were used. The relationship between E_{dif} and the concentration

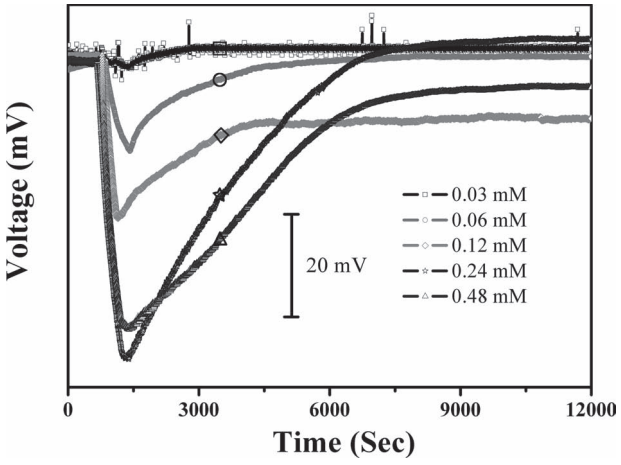

Figure 2. Time-course changes of membrane potentials for the photoelectric conversion system measured in darkness and UV irradiation of different concentration of MGCB solutions with a fixed incident light intensity and environment temperature (T = 25 °C, I_s = 375 mW/cm^2).

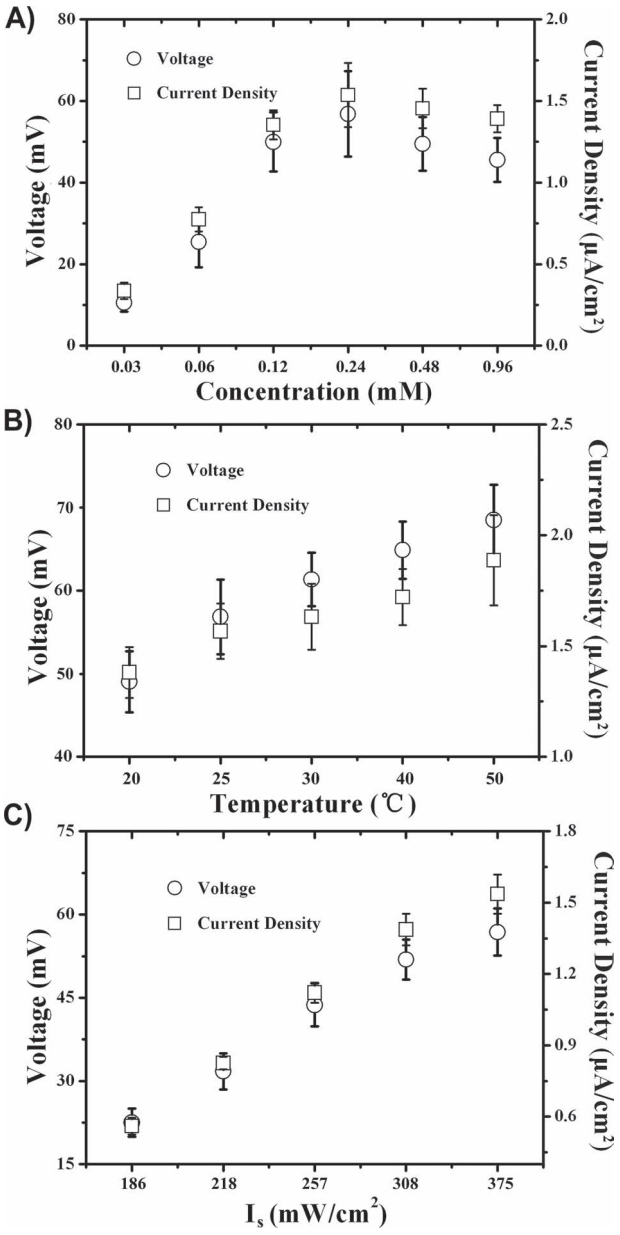

Figure 3. Power generate from hydroxide ion-driven nanofluidic channels. Both the photocurrent and membrane potentials are influenced by the concentration of MGCB (A), environmental temperature (B), and incident light intensity (C). The tip side of the channels used in our system before modification was ≈10 nm. The symbols in each panel stand for photocurrent (grey squares) and membrane potential (black circles).

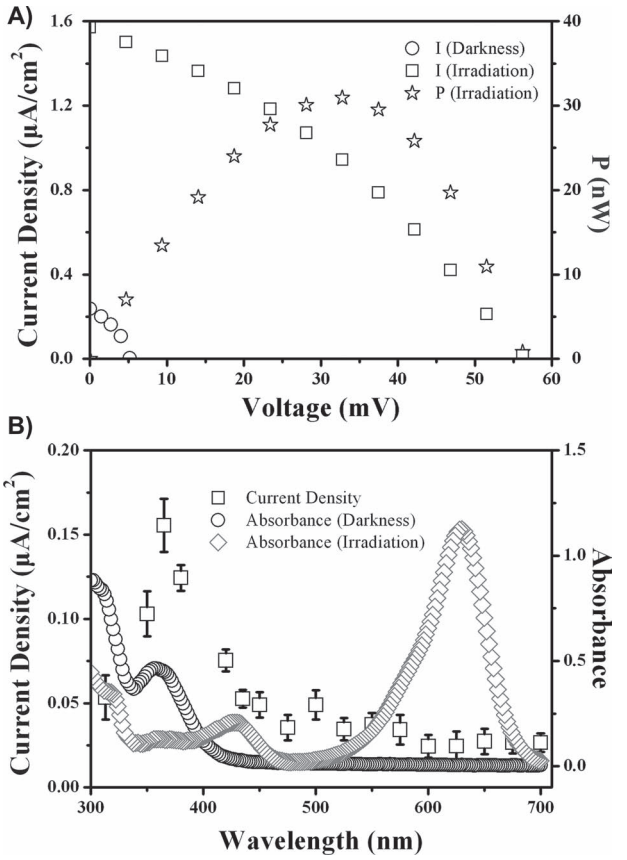

Figure 4. Photoelectrical properties. a) *J–V* characteristics of the optimized photoelectric conversion system with incident light intensity of 375 mW/cm^2. b) Action spectrum of the MGCB photoresponse. The black circles and grey squares represent the absorption spectra of MGCB prior and after UV irradiation, while the black squares represent the magnitude of the light-induced transient responses. The interference filters were used to provide an actinic light of wavelengths (±10 nm).

of MGCB (C_{MGCB}) as well as the relationship between I_p and the C_{MGCB} were shown in **Figure 3**A (T = 25 °C; I_s = 375 mW/cm^2). As shown, E_{dif} and I_p dramatically increased in the range from 0.03 mM to 0.24 mM and reached the maximum values at the concentration of 0.24 mM. The maximum values of E_{dif} and I_p were ≈56.5 mV and ≈1.57 μA/cm^2, respectively. If the C_{MGCB} continuously increased, E_{dif} and I_p would decline slowly. Because in the concentrated solution, the continuously increasing hydroxide ions would simultaneously increase the interaction between the hydroxide ions and cations, which could produce negative impacts on anions diffusion and decrease the power generation. In our system, the maximum values of E_{dif} and I_p were obtained when the concentration of MGCB was 0.24 mM. The influences from temperature (Figure 3B) and light intensity (I_s) (Figure 3C) on the photoelectric conversion behavior have also been studied. Both E_{dif} and I_p increased with the environmental temperature and light intensity. This is because heating can decrease the resistance of solution and increase the movement of ions. And high-intensity light can make photochemical reaction easy and thorough.

Figure 4A showed the optimized current–voltage (*J–V*) characteristics of the photoelectric conversion under certain conditions (C_{MGCB} = 0.24 mM, T = 25 °C, I_s = 375 mW/cm^2). The device exhibited a property of ionic current rectification under irradiation with short circuit current (I_{sc}) of 1.56 μA/cm^2 and opened circuit potential (V_{oc}) of 56.7 mV. It should be pointed out that the V_{oc} in ideal cases is equal to the diffusion potential difference, and therefore depends directly on the hydroxide ion concentration gradient and the transport number of the ions forming the diffusing electrolyte, while the I_{sc} depends on the concentration of redox couple in this diffusing electrolyte. With the present experimental setup

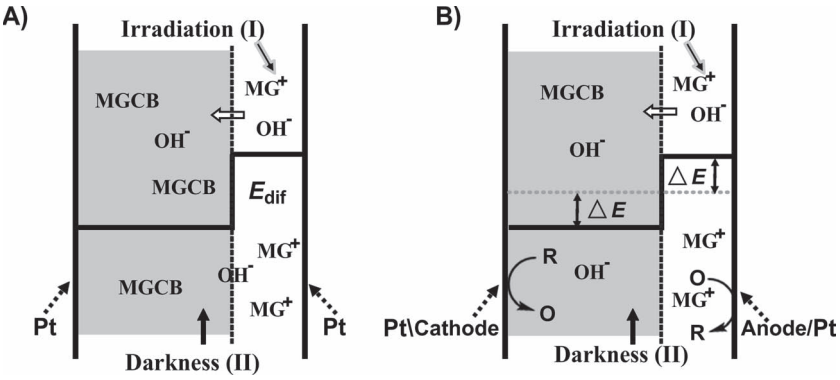

Figure 5. a) Schematic representation of the E_{dif} in part of PEC under the condition of V_{oc}. When the MGCB was irradiated, the generated hydroxide ions would transport across the smart gating hydroxide ion-driven nanochannel from the irradiation side (I) to the darkness (II) under the force of concentration gradients and contributed to the E_{dif}. b) Schematic representation of the electrode potential difference in the part of PEC under the condition of J_{sc}. Before irradiation, no ionic concentration gradients occurred and the potentials on both sides of electrodes were same, as a result no electron flowed through the external circuit. After irradiation, the E_{dif} occurred and the I_p generated by redox reactions on electrodes.

the maximum measured power $(IV)_{max}$ is 30.94 nW, from which we can determine the power efficiency η_e. It was defined as the ratio of the input power P_{in}, in the form of light radiation (I_s), to the output power P_{out} in the form of electrical energy:

$$\eta_e = \frac{P_{out}}{P_{in}} = \frac{(IV)_{max}}{I_s} \tag{1}$$

The values could be calculated according to the Equation (1), which was around 0.00825%. Because the photo-induced pH changes reflect the electrical activity signal of MGCB molecules, narrow band filters were used to obtain an action spectrum of the current signals. Figure 4b showed the action spectrum (open square) represented as the normalized peak current density. A peak maximum (λ_{max}) of 365 nm was obtained. For comparison, an absorption spectrum of MGCB molecules in dilute solution was taken and plotted as blue circles. The characteristic maximum absorbance of MGCB molecules was at 358 nm. Apparently, the maximum absorbance of MGCB molecules was basically at the same position as the peak of photocurrent generation. This agreement illustrated that the photocurrent stemmed from the molecule MGCB.

Figure 5 showed the principle of the photoelectric conversion. When the MGCB was irradiated, the generated OH^- would transport across the smart gating hydroxide ion-driven nanochannel membrane from the irradiation side (part I) to the dark side (part II) under the force of concentration gradients. The transported ions would then cause the charge imbalance on both sides of the membrane and generate the E_{dif} (Figure 5a) whose values could be calculated by measuring the pH under the conditions of darkness and irradiation according to the following Equation (2):

$$E_{dif} = E^I - E^D = \left(E^{I\theta} + \frac{RT}{zF}\ln\frac{\alpha^I_{ox}}{\alpha^I_{red}}\right) - \left(E^{D\theta} + \frac{RT}{zF}\ln\frac{\alpha^D_{ox}}{\alpha^D_{red}}\right) \tag{2}$$

Where E^I and E^D are electrode potentials at each side of irradiation and darkness respectively, R is the gas constant, T is the absolute temperature (K), F is the Faraday constant, and α^I_{red} and α^I_{red} are activities of the products that exist in the irradiation and dark side of the cell. To hydrogen electrode, $E^{I\theta}$ and $E^{D\theta}$ were equal to zero, thus Equation (2) could be substituted with Equation (3):

$$E_{dif} = E^I - E^D = \frac{RT}{F}\ln\frac{\alpha^I_{H^+}\alpha^D_{H_2}}{\alpha^I_{H_2}\alpha^D_{H^+}} \tag{3}$$

In order to simplify the calculation process, $\alpha^I_{H_2}$ and $\alpha^D_{H_2}$ could be removed from Equation (3). As a result, Equation (4) was finally obtained:

$$E_{dif} = 0.059\lg\frac{\alpha^I_{H^+}}{\alpha^D_{H^+}} = 0.059(pH^I - pH^D) \tag{4}$$

E_{dif} could be calculated according to the Equation (4) by measuring the pH under the condition of darkness and irradiation. In this experiment, the pH values were 6.9 (darkness) and 8.5 (under irradiation), from which we calculated the maximum voltage of 94.4 mV (absolute value). In this case, the efficiency can be calculated according to the following equation:

$$\eta_e = \frac{P_{mea}}{P_{Cal}} = \frac{IV_{mea}}{IV_{cal}} = \frac{V^2_{mea}/R}{V^2_{cal}/R} = \frac{V^2_{mea}}{V^2_{cal}} \tag{5}$$

where P_{mea} and P_{cal} are the measured and calculated power, corresponding to the measured and calculated voltages, from which we can calculate its efficiency η_e; the value was around 36.08%. After cutting off UV irradiation, the diffusion potential E_{dif} would gradually diminish until it reached zero and a homogeneous solution was obtained. As to I_{sc}, the two electrode potentials were forced to be equal by releasing or accepting electrons that were generated by redox reactions on both electrodes. This process could be illustrated in Figure 5b. Before irradiation, no ions concentration gradients occurred and the potentials on both sides of membrane were the same, thus no electrons flowed through the external circuit.

As the chemical concentration gradient is a type of Gibbs free energy available, ion diffusion process is from a high-concentrated (H) solution to a low-concentrated (L) solution. The two bulk reservoirs are interconnected with nanochannels under certain surface charge properties. In an infinitesimal time unit (dt), the Gibbs free energy loss (dG) due to solution mixing can be described as:

$$dG = -\frac{RT}{nF}\ln\frac{\alpha_H}{\alpha_L}(|I_+| + |I_-|)\,dt \tag{6}$$

where $\alpha_{H/L}$ is the chemical activity of the ion species on the H (irradiation) or L (darkness) side, and $I_\pm$ is the ion flux contributed to by either cations (+) or anions (−). During the diffusion

process, owing to the asymmetric diffusion between cations and anions, part of the Gibbs free energy could be converted into electric work (dW) in the form of a net diffusion current:

$$dW = \frac{RT}{nF} \ln \frac{\alpha_H}{\alpha_L} \frac{(|I_+| - |I_-|)^2}{|I_+| + |I_-|} dt \quad (7)$$

In this case, the energy conversion efficiency can be derived as:

$$\eta = \left| \frac{dW}{dG} \right| = \left(\frac{|I_+| - |I_-|}{|I_+| + |I_-|} \right)^2 \quad (8)$$

As the total ion diffusion through the nanochannel in an infinitesimal time unit could be scaled by the absolute diffusion current which contributed by both cations and anions ($|I_+| + |I_-|$), only the net diffusion current ($|I_+| - |I_-|$) generated from the asymmetric ion diffusion across the nanochannel can be harvested as electric work. Because such an energy conversion system that are based on the ion transport can be described by the Poisson-Nernst-Planck (PNP) equations,[6c,d,17] the values of $(|I_+| - |I_-|)/(|I_+| + |I_-|)$ are correlated with the electrolyte concentration,[17] the η_e can be substituted by the equation below:

$$\eta = \left| \frac{dW}{dG} \right| = \left(\frac{|I_+| - |I_-|}{|I_+| + |I_-|} \right)^2 = \left(\frac{\Delta C}{C_D} \right)^2 \quad (9)$$

The average (Donnan) concentration, C_D, represents the total concentration of ions inside the charged nanochannel at equilibrium, and ΔC represents the concentration of negative ions drops from $C_{irradiation}$ to $C_{darkness}$. In this case, the efficiency η_e can be calculated to have a value around 35.73%.

3. Conclusions

In summary, inspired by retina in living system that can serve as a light-driven cross-membrane proton pump, a photoelectric conversion system which can work in a alkaline condition based on a smart gating hydroxide ion-driven nanofluidic channel and photo-induced reversible pH changes MGCB has been demonstrated. Experimentally, the membrane potential, photocurrent, and the resulting electrical power were very sensitive to the external and internal conditions. For the external conditions, the electrical power always increased with increasing temperature and light intensity. For the internal conditions, such as the concentration of MGCB, CTAB, and pH, this trend could not be obtained because output power was decided by many factors including static interactions, ion mobility, and the conditions of chemical reaction. The conversion performances in this energy conversion system were 0.00825% and 36%, which we calculated using the techniques of photoelectric conversion and Gibbs free energy diffusion, respectively. The study suggests that the electric power generation and its performance can be further optimized by selecting appropriate photosensitized molecules and enhancing the surface-charge density as well as adopting the appropriate channel size. This facile, cost-efficient, and environmentally friendly photoelectric conversion system has potential applications for future energy demands. Based on the progress of photoelectric conversion systems of photoinduced reversible pH changes and previous light-driven proton pump,[2b] the coming development photoelectric conversion system would work under a full range of pH conditions, from pH 1 to 14.

4. Experimental Section

Optical Properties: UV-vis absorption spectra provided some information on the occurrence of chemical reaction and their corresponding transition process. Figure 4b displayed the normalized absorption of MGCB (black circle) and their corresponding products (Grey Square). With visible irradiation, MGCB had little dissociation and showed an absorption peak at about 358 nm. After UV irradiation, MGCB released hydroxide ions easily and formed MG cations, whose absorption spectra were different from the original MGCB molecule, giving rise to two new absorption peaks occurred at 428 and 630 nm. These results were recorded with a JASCO V-570 spectrophotometer.

Nanochannel Fabrication: The conical nanochannels were prepared with polyethylene terephthalate (PET, 12 μm thick, ≈10^{-7} to 10^{-8} ion tracks/cm^2) membrane, which was irradiated with single swift heavy ion (Au) of energy 11.4 MeV per nucleon at the UNILAC linear accelerator (GSI, Darmstadt, Germany). After UV irradiation for 1 h on each side, the polymer membrane was subsequently chemical etched at room temperature (about 295 K) from one side with 9 M NaOH, whereas the other side of the cell contains acidic solutions (1 M KCl and 1 M HCOOH), which can neutralize the etchant as soon as the pore opens (see Supporting Information Figure S1). For the process of etching, the current was used to monitor the etchant degree. After the etching finished, the membrane was soaked in MilliQ water (18.2 MΩ) to remove residual salts. The large opening of the conical nanochannel was called base, while the small opening was called tip. The diameter of the base was estimated from the bulk etch rate measured in parallel etching experiments. The tip diameter was evaluated by an electrochemical measurement of the ionic conductance of the nanochannel filled with 1 M KCl solution as electrolyte via the following equation:

$$d_{tip} = \frac{4LI}{\pi k(c) U D} \quad (10)$$

where d_{tip} is the tip diameter, D is the base diameter, and $k(c)$ is the special conductivity of the electrolyte. For 1 M KCl solution at 25 °C $k(c)$ was 0.11173 Ω^{-1} cm^{-1}. L is the length of the channel, which could be approximated to the thickness of the membrane after chemical etching. U and I are the applied voltage and measure ionic current in the pore conductivity measurement respectively. In this work, the base diameter was usually several hundred nanometers and the tip diameter was around 10 nm.

Nanochannel Functionalization: The chemical reaction scheme for the conversion of carboxyl into amino terminated groups is given in Scheme 1C. For the activation of carboxyl groups, pentafluorophenol was used for activation instead of *N*-hydroxysuccinimide because pentafluorophenyl esters are ≈10 times more active than the corresponding *N*-hydroxysuccinimidyl esters. For the activation of the carboxyl groups into pentafluorophenyl esters (II), an ethanol solution containing *N*-(3-dimethylaminopropyl)-*N*′-ethylcarbodiimide hydrochloride (EDC, 100 mM) and pentafluorophenol (PFP, 200 mM) was placed on both sides of the track-etched single channel membrane. The reaction was carried out for 1 h at room temperature. Then the solution was replaced with ethylendiamine (EDA, 100 mM) on both sides of the membrane for an overnight time period in order to get amino (–NH_2) terminated groups. Finally, the chemically modified membranes were washed with ethanol and then with distilled water.

Current–Voltage Recordings: The current and voltage were measured by connecting a Keithley 6487 picoammeter (Keithley Instruments, Cleveland, OH) and a Keithley 2182A nanovoltmeter (Keithley Instruments, Cleveland, OH) at room temperature. Platinum electrodes

were used as working electrode and counting electrode where redox reactions occurred and the Pt electrode area was 0.10 cm^2. The process and conditions of all the measurements mentioned in this article are of the same, if no particular instructions were added on. And each test was repeated 5 times to obtain the average number value.

Supporting Information

Supporting Information is available from the Wiley Online Library or from the author.

Acknowledgements

The authors thank the financial support by National Research Fund for Fundamental Key Projects (2012CB933200, 2011CB935703, 2010CB934700), National Natural Science Foundation (21171171, 20920102036, 21121001, 91127025), and the Key Research Program of the Chinese Academy of Sciences (KJZD-EW-M01).

Received: November 6, 2012
Revised: November 20, 2012
Published online: January 16, 2013

[1] a) M. Altamirano, *J. Cell. Physiol.* **1955**, *46*, 249; b) R. H. Garrett, C. M. Grisham, *Biochemistry 2nd ed.*, Saunders College Publishing, Philadelphia **1999**, Ch. 5; c) D. Gust, T. A. Moore, A. L. Moore, *Acc. Chem. Res.* **2000**, *34*, 40; d) D. A. LaVan, J. N. Cha, *Proc. Natl. Acad. Sci. USA* **2006**, *103*, 5251.

[2] a) J. Xu, D. A. Lavan, *Nat. Nanotechnol.* **2008**, *3*, 666; b) L. Wen, X. Hou, Y. Tian, J. Zhai, L. Jiang, *Adv. Funct. Mater.* **2010**, *20*, 2636; c) W. Guo, L. Cao, J. Xia, F.-Q. Nie, W. Ma, J. Xue, Y. Song, D. Zhu, Y. Wang, L. Jiang, *Adv. Funct. Mater.* **2010**, *20*, 1339; d) D. Stein, M. Kruithof, C. Dekker, *Phys. Rev. Lett.* **2004**, *93*, 035901; e) D. Gillespie, *Nano Lett.* **2012**, *12*, 1410.

[3] a) L. Wen, Y. Tian, J. Ma, J. Zhai, L. Jiang, *Phys. Chem. Chem. Phys.* **2012**, *14*, 4027; b) X. Hou, W. Guo, L. Jiang, *Chem. Soc. Rev.* **2011**, 2385; c) X. Hou, L. Jiang, *ACS Nano* **2009**, *3*, 3339; d) S. Howorka, Z. Siwy, *Chem. Soc. Rev.* **2009**, *38*, 2360; e) M. Zhang, X. Hou, J. Wang, Y. Tian, X. Fan, J. Zhai, L. Jiang, *Adv. Mater.* **2012**, *24*, 2424; f) X. Hou, H. Zhang, L. Jiang, *Angew. Chem. Int. Ed.* **2012**, *51*, 5296.

[4] a) S. Wen, T. Zeng, L. Liu, K. Zhao, Y. Zhao, X. Liu, H.-C. Wu, *J. Am. Chem. Soc.* **2011**, *133*, 18312; b) Z. S. Siwy, M. Davenport, *Nat. Nanotechnol.* **2010**, *5*, 174; c) Z. Chen, Y. Jiang, D. R. Dunphy, D. P. Adams, C. Hodges, N. Liu, N. Zhang, G. Xomeritakis, X. Jin, N. R. Aluru, S. J. Gaik, H. W. Hillhouse, C. Jeffrey Brinker, *Nat. Mater.* **2010**, *9*, 667; d) D. K. Lathrop, E. N. Ervin, G. A. Barrall, M. G. Keehan, R. Kawano, M. A. Krupka, H. S. White, A. H. Hibbs, *J. Am. Chem. Soc.* **2010**, *132*, 1878; e) C. Dekker, *Nat. Nanotechnol.* **2007**, *2*, 209; f) C. R. Martin, Z. S. Siwy, *Science* **2007**, *317*, 331; g) B. Zhang, Y. Zhang, H. S. White, *Anal. Chem.* **2004**, *76*, 6229; h) A. de la Escosura-Muñiz, A. Merkoçi, *ACS Nano* **2012**, *6*, 7556.

[5] E. N. Savariar, K. Krishnamoorthy, S. Thayumanavan, *Nat. Nanotechnol.* **2008**, *3*, 112.

[6] a) P. Banerjee, I. Perez, L. Henn-Lecordier, S. B. Lee, G. W. Rubloff, *Nat. Nanotechnol.* **2009**, *4*, 292; b) F. H. J. van der Heyden, D. J. Bonthuis, D. Stein, C. Meyer, C. Dekker, *Nano Lett.* **2007**, *7*, 1022; c) F. H. J. van der Heyden, D. J. Bonthuis, D. Stein, C. Meyer, C. Dekker, *Nano Lett.* **2006**, *6*, 2232; d) F. H. J. van der Heyden, D. Stein, C. Dekker, *Phys. Rev. Lett.* **2005**, *95*, 116104.

[7] Y. B. Xie, X. W. Wang, J. M. Xue, K. Jin, L. Chen, Y. G. Wang, *Appl. Phys. Lett.* **2008**, *93*, 163116.

[8] a) S. P. Balashov, E. S. Imasheva, V. A. Boichenko, J. Anton, J. M. Wang, J. K. Lanyi, *Science* **2005**, *309*, 2061; b) W. Kühlbrandt, J. Zeelen, J. Dietrich, *Science* **2002**, *297*, 1692; c) W. Kühlbrandt, *Nature* **2000**, *406*, 569; d) S. Subramaniam, R. Henderson, *Nature* **2000**, *406*, 653; e) R. H. Lozier, R. A. Bogomolni, W. Stoeckenius, *Biophys. J.* **1975**, *15*, 955.

[9] M. Iwamoto, K. Shimono, M. Sumi, K. Koyama, N. Kamo, *J. Phys. Chem. B* **1999**, *103*, 10311.

[10] a) Y. Jin, T. Honig, I. Ron, N. Friedman, M. Sheves, D. Cahen, *Chem. Soc. Rev.* **2008**, *37*, 2422; b) C. Horn, C. Steinem, *Biophys. J.* **2005**, *89*, 1046; c) T. Miyasaka, T. Atake, T. Watanabey, *Chem. Lett.* **2003**, *32*, 144; d) T. Miyasaka, K. Koyama, *Electrochemistry* **2000**, *68*, 865; e) Y. Saga, T. Watanabe, K. Koyama, T. Miyasaka, *J. Phys. Chem. B* **1999**, *103*, 234; f) B. Robertson, E. P. Lukashev, *Biophys. J.* **1995**, *68*, 1507.

[11] a) M. Irie, *J. Am. Chem. Soc.* **2002**, *105*, 2078; b) L. Wen, J. Ma, Y. Tian, J. Zhai, L. Jiang, *Small* **2012**, *8*, 838; c) H. Liu, Y. Xu, F. Li, Y. Yang, W. Wang, Y. Song, D. Liu, *Angew. Chem. Int. Ed.* **2007**, *46*, 2515.

[12] R. N. Macnair, *Photochem. Photobiol.* **1967**, *6*, 779.

[13] M. Xu, D. Liu, H. C. Allen, *Environ. Sci. Technol.* **2006**, *40*, 1566.

[14] Z. S. Siwy, *Adv. Funct. Mater.* **2006**, *16*, 735.

[15] Y. Jin, N. Friedman, M. Sheves, T. He, D. Cahen, *Proc. Natl. Acad. Sci. USA* **2006**, *103*, 8601.

[16] a) C. Ma, G. Li, Y. Xu, H. Wang, X. Ye, *Colloids Surf. A* **1998**, *143*, 89; b) G. Rong, L. Wei-Ya, F. Guo-Kang, *Acta Phys.-Chim. Sin.* **2001**, *17*, 1062.

[17] I. Vlassiouk, S. Smirnov, Z. Siwy, *Nano Lett.* **2008**, *8*, 1978.